Modeling Aggregate Interference with Heterogeneous Secondary Users and Passive Primary Users for Dynamic Admission and Power Control in TV Spectrum

Zhongyuan Zhao and Mehmet C. Vuran
Cyber-Physical Networking Lab
Computer Science and Engineering
University of Nebraska-Lincoln, Lincoln, Nebraska, USA
{zhzhao,mcvuran}@cse.unl.edu

***Abstract*—Interference management in current TV white space and Citizens Broadband Radio Service networks is mainly based on geographical separation of primary and secondary users. This approach overprotects primary users at the cost of available spectrum for secondary users. Potential solutions include acquiring more primary user information, such as a measurement-enhanced geographical database, and cooperative primary user, such as the TV set feedback in the next generation TV systems. However, one challenge of these solutions is to effectively manage the aggregate interference at TV receivers from interweaving secondary users. In this paper, a stochastic geometry-based aggregate interference model is developed for unlicensed spectrum shared by heterogeneous secondary users that have various transmit powers and multi-antenna capabilities. Moreover, an efficient computation approach is presented to capture network dynamics in real-time via a down-sampling that preserves high-quantile precision of the model. The stochastic geometry-based model is verified experimentally in ISM band. It is shown that the model enables separate control of admission and transmit power of multiple co-located secondary networks to protect primary users and maximize spectrum utilization.**

***Index Terms*—Cognitive Radio Networks, Outage Analysis, TV Black Space, TVWS, Stochastic Geometry, Power Control**

I. Introduction

Interference management in Cognitive Radio Networks (CRNs) such as TV white space (TVWS) [1] and Citizens Broadband Radio Service (CRBS), is based on database-driven dynamic spectrum access (DSA) with geographical separation of primary users (PUs) and secondary users (SUs) [2]. Geographical separation limits the benefits of CRNs in many populated metropolitan cities (TVWS) [3], [4], and coastal cities (CRBS) [2], where spectrum crisis is mostly experienced [5]. Several approaches are proposed to reduce the geographical separation. Measurement-enhanced spectrum databases [6] enable Fine-Grained TVWS (FG-TVWS) in urban environments, such as indoors and building-shadowed areas. Moreover, TV set-assisted DSA enables SUs to access active legacy TV channels, namely TV black-space (TVBS), by leveraging the activity of TV receivers [4], [7]. TVBS access becomes more feasible with the recent developments in legacy systems. For example, ATSC 3.0 [8], standardizes TV set feedback to enable interactive and personalized services.

A major challenge of FG-TVWS and TVBS is to manage the interference from SUs to PUs (TV receivers). Restrictions such as guard zone and individual SU footprint limit are insufficient to protect PUs exposed to aggregated interference from a number of SUs, especially given the favorable propagation conditions in TV band. To address this problem, a spectrum manager (global or local) is envisioned to schedule the DSA of SUs and manage the interference (Fig. 1). The spectrum manager is assumed to have real-time and/or statistical information of both PUs and SUs. Based on network dynamics, the spectrum manager can adaptively control the admission and transmit power of SUs to manage the aggregated interference.

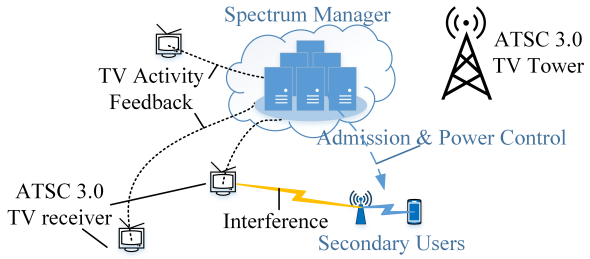

Fig. 1. Spectrum management architecture for enhanced TV spectrum access.

Aggregate interference can be obtained through cooperative spectrum sensing [6], [9], and PU feedback, at the cost of overhead in spectrum, backhaul, and energy. Its accuracy depends on spatial sampling [6]. A parallel approach is statistical modeling. Theoretical aggregate interference models [10]–[17] mostly consider homogeneous transmitter profile, which makes it difficult to manage spectrum shared by multiple SU networks with different transmit power, density, and multi-antenna profiles, such as WiFi, Bluetooth, Internet of Things, Body Area Networks. Another challenge is to achieve accuracy with low computational complexity. Moment matching-based Lognormal approximation [18], has significant errors in outage analysis, and is inconsistent under network dynamics, as shown in Section V. Sophisticated models [10]–[17] require high computational complexity for large dynamic range of interference power, and could not capture heterogeneous SUs.

In this paper, an analytical interference model is developed for scenarios in which spectrum is shared by passive PUs (no transmitter) and co-located SUs with heterogeneous transmitter profiles. Our contributions include: 1) We extend existing models from unified transmitter profile to multiple classes of transmit powers and Multiple Input Multiple Output (MIMO) capabilities, under class-specific admission and power control policies. 2) An efficient computation approach is developed

to evaluate existing stochastic geometry-based models in real-time for large dynamic range of interference power. 3) To the best of our knowledge, we conduct the first empirical validation of the key modeling components shared by ours and existing works [10]–[17]. The developed interference model and efficient computation approach can potentially enhance DSA techniques in TV band.

The rest of this paper is organized as follows: Related work is discussed in Section II. System model is introduced in Section III. In Section IV, the aggregate interference model, admission and power control, and efficient computation approach are introduced. Simulation and experiment results are presented in Sections V and VI, respectively. Finally, the paper is concluded in Section VII.

II. Related Work

A. TV Spectrum Management

Spectrum management in TVWS is mainly database-driven: available channels are estimated based on radio propagation models [3], and an SU queries the database with its geolocation and radio profile (device type specified by antenna height and transmit power [2]) for a list of available channels. Geolocation database is extended to a 3-tier Spectrum Access System (SAS) in CBRS that prioritize SUs of different tiers with admission control [2]. Interference in TVWS and CBRS is managed through geographical separation of PU and SU based on a prescribed protection zone, and SU device types.

To address the over-protection of PU caused by the limits of propagation model [3], spectrum sensing-enhanced geolocation database (radio environment map) [6] is developed to exploit FG-TVWS caused by shadowing of terrain. On the other hand, cooperative PU-based TVBS access [4], [7] requires real-time spectrum scheduling of SUs based on activities of neighboring TV receivers. These approaches reduce the geographical separation with more PU information.

Existing approaches mainly focus on PU information, while leaving interference analysis in a static (e.g. worst case) approach. However, for FG-TVWS and TVBS, static analysis may not effectively enable sufficient spectrum for SUs while protecting PU. This work extends estimation of available channels from relying only on PU information to the activity dynamics of SUs. Consequently, spectrum utilization can be improved by adaptively controlling the admission and transmit power of SUs based on network dynamics.

B. Stochastic Geometry-Based Interference Model

Modeling unplanned wireless networks is based on stochastic geometry [10]. In this framework, aggregate interference is modeled as a random sum of independent and identically distributed (i.i.d.) individual interference (random interference) emitted from transmitters following a Poisson Point Process (PPP). With uniform transmit power and known transmitter density, the characteristic function (CF) of aggregate interference from Poisson transmitters is obtained from the CF of the random interference. The first two moments are found by Compbell's theorem [18]. In [11], the interference model is extended to CRNs with power control, contention, and their hybrids. However, only a single PU receiver is considered in [11], which limits it to low-PU-density scenarios.

In tiered networks, such as CRNs [12], Device-to-Device (D2D), and Heterogeneous Networks (HetNets) [14], different user tiers are modeled as independent PPPs. Transmitters restricted by contention, repulsion, and guard zones, are modeled as Hard Core Point Process (HCPP), Poisson Hole Process (PHP) [12], [13], and their combinations [14]. Low-tier transmitter follows a PHP, which has no known closed-form model, but has closed-form bounds [14] and PPP-approximated models [12]. However, these works only consider the single antenna case. Individual MIMO interference is modeled in [19]. MIMO aggregate interference is modeled for cellular [15] and HetNets [16], and CRNs [17]. In [17], massive MIMO and power control are considered with a cellular-like PU network, which is not applicable for TV spectrum with passive PUs. Interference model in CRNs without stochastic geometry [20] is limited by the need of instantaneous user density.

For spectrum management, existing models face three challenges. First, unlicensed spectrum is shared by multiple networks with different capabilities and of dynamic composites, which is not captured by existing models. Based on the underlying model in [10], [11], and the approach of modeling multiple PUs and SUs in [12]–[14], [17], our model is able to track interference in spectrum shared by peer networks with heterogeneous transmit powers and MIMO capabilities.

The second challenge is the computational complexity. The CF manipulation-based underlying mathematics [10] requires (Inverse) Fourier Transform(s) in linear-domain. To cover a total dynamic range of 120 dB individual and aggregated interference, a sample size $n = 10^{12}$ is required for linear-domain functions, such as CFs and PDFs. This prohibits real-time evaluation of existing models, which has a time complexity of $\mathcal{O}(n \log(n))$ and a space complexity of $\mathcal{O}(n)$. The efficient computation approach introduced in Section IV-D reduces the required sample size by 10^5 and enables sub-second estimation, which opens the door for interference model-assisted real-time spectrum management.

Third, to the best of our knowledge, there is no empirical validation of the underlying mathematics of ours and existing works [10]–[17], due to the difficulty of involving numerous transmitters. A theory without empirical evidence might not persuade any reforms in spectrum policy, which involves various stakeholders. In Section VI, we present empirical validation results for this shared baseline theory.

III. System Model

We consider a CRN with numerous PUs and SUs. Their activities and locations are known to a spectrum manager (Fig. 1). First, an SU has to be admitted by the spectrum manager. Then, the admitted SUs access the spectrum via contention over-the-air (OTA) or within the spectrum manager.

A. Point Process Modeled Network

The primary network is consider as a broadcast network, where PU is a passive receiver (e.g. OTA TV receivers). To

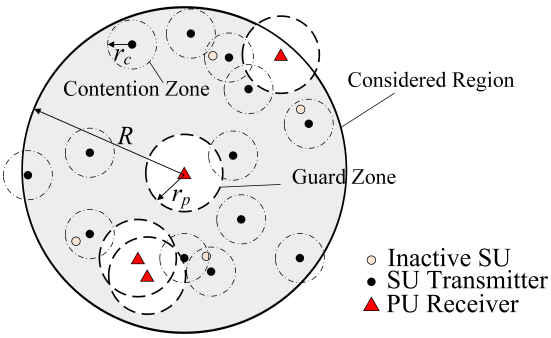

Fig. 2. TV band CRN model with PU guard zone and SU contention.

model interference, a finite region with radius R centered on an arbitrary PU is considered (Fig. 2). PUs and SUs are modeled as two independent homogeneous Poisson Point Processes (PPP) with densities λ_p and λ_s, respectively. There is no minimum distance between PUs. Guard zone is a disk centered on PU in which SU is not allowed to transmit. With guard zones, SU transmitters are modeled as a Poisson Hole Process (PHP) [13]. Moreover, SUs access spectrum based on contention, which is modeled as a Hard Core Point Process (HCPP). The radius of contention zone is r_c, and the radius of PU guard zone is r_p. High traffic demand of SU is assumed so that it will access the spectrum whenever possible.

The retention ratio of SU after the guard zone of PU equals to the chance of no PU located within a distance of r_p from SU, which can be found from Nearest Neighbor Function:

$$q_p = \exp\left(-\lambda_p \pi r_p^2\right) \ . \tag{1}$$

The approximated retention ratio of SU contention, modeled as a HCPP, is found in [11], [14]. SU transmitter as PHP overlaid on HCPP is approximated by two independent thinning processes on the underlying PPP of density λ_s [11], [14].

The spectrum can be shared by heterogeneous SUs with different throughput and QoS requirements, and radio capabilities. Heterogeneous SUs are modeled as K independent classes of SUs, where an SU class k has a density λ_{sk}, transmit power p'_k, and certain MIMO capability (e.g. single v.s. multiple antenna(s)), where $k \in \{1 \dots K\}$, and $\lambda_s = \sum_{k=1}^{K} \lambda_{sk}$. Admission and transmit power control can be class-specific, in order to maximize spectrum utilization.

B. Radio Propagation

Consider path loss and composite shadowing and fading, the received power, $y(d)$, at distance d from a transmitter is:

$$y(d) = p \cdot l(d) \cdot h \ , Y(d) = P + L(d) + H \ , \tag{2}$$

where p is the emission power of transmitter, $l(d)$ is path gain, and h is fading. As a convention, their logarithmic counterparts are denoted by capitalized symbols $Y(d)$, P, $L(d)$, and H in (2). The path gain function is:

$$l(d) = l_0 d^{-\beta} \ , L(d) = L_0 - 10\beta \log_{10}(d) \ , \tag{3}$$

where l_0 and L_0 are the reference path gains in linear and logarithmic domains, respectively.

IV. Aggregate Interference Model

We first introduce the mathematical framework of interference from a single SU class, then extensions are provided for MIMO, and multiple SU classes. Next, a power control scheme based on the interference model is presented, followed by an efficient computational approach.

A. Interference from a Single SU class

The aggregate interference u is modeled as the sum of N i.i.d. random variables (r.v.s), y, which is the interference from a random transmitter in the considered region. Since SU transmitters are modeled as a PPP, N follows Poisson distribution. The characteristic function (CF) of u is [10], [11]:

$$\Phi_u(w) = exp\left\{\lambda_t c \Phi_y(w)\right\} \ , \tag{4}$$

where λ_t is SU transmitter density, $c = \pi(R^2 - r_p^2)$ is the area of considered region, and the CF of y is [11]:

$$\Phi_y(w) = \int_0^\infty \int_0^\infty f_h(h) f_p(p) \Phi_l(wph) \mathrm{d}p \mathrm{d}h \ , \tag{5}$$

where $f_h(x)$ and $f_p(x)$ are the PDFs of channel fading and emission power toward PU, respectively. The PDF of an uniform-distributed random transmitter located at distance, d, from the origin point is $f_d(d) = \frac{2\pi d}{c}$, where $r_p \le d \le R$ [11]. The PDF of path gain l from a random transmitter is

$$f_l(l) = \frac{2\pi}{c\beta} l_0^{\frac{2}{\beta}} l^{(-\frac{2}{\beta}-1)} \text{ , where } l(r_p) \ge l \ge l(R) \ , \tag{6}$$

its CF is found by Fourier Transform $\Phi_l(w) = \mathcal{F}\left\{f_l(l)\right\}(w)$.

We consider a limited scattering environment for MIMO while leaving the rich scattering environment for future work. An SU has an m-antenna array, $b \le m$ streams, and transmit power of p'. The communication and interference channels are uncorrelated, and noise is unknown. Transmitted signal for each stream on the m antennas is assumed to be a complex Gaussian random vector $\sim \mathcal{CN}(0, \frac{p'}{mb})$ [15], [16], [19]. For each stream, the emission power follows $\mathbf{Exponential}(b/p')$, and the total emission power p follows a scaled Chi-square distribution $\sqrt{\frac{p'}{b}}\chi_b^2$ with b degrees of freedom.

B. Multiple SU Classes

To control SU density, the spectrum manager admits an arriving SU at probability ρ. Admission control is modeled as an independent thinning process on the PPP of SU with retention ratio ρ. The density of admitted SUs is $\rho\lambda_s = \sum_{k=1}^{K} \rho_k \lambda_{sk}$, where ρ_k is the admission probability of SU class k.

Assume a fair, identical contention across all SU classes, based on the retention probability of SU contention given in [11], the density of class k SU transmitter is:

$$\lambda_{tk}(d) \begin{cases} \approx \frac{q_p \rho_k \lambda_{sk}\left[1-\exp\left(-\rho\lambda_s \pi r_c^2\right)\right]}{\rho\lambda_s \pi r_c^2} \ , & d \ge r_p \\ = 0, & d < r_p \end{cases} . \tag{7}$$

With CF of single SU class interference, $\Phi_{sk}(w)$, from (4), the CF of interference from heterogeneous SUs, us, is [21]:

$$\Phi_{us}(w) = \prod_{k=1}^{K} \Phi_{uk}(w) \ . \tag{8}$$

Compared to using a PDF of emission power for all SU classes [11], (7) and (8) can track interference from each SU class, and further incorporate interference from and to adjacent channels based on the emission mask of SU transmitter.

C. Secondary User Power Control

The CF of Signal-to-Interference Ratio (SIR) of PU, γ, is

$$\Phi_\gamma(w) = \int_0^\infty f_\zeta(x)\Phi_u(wx)dx \ , \tag{9}$$

where $f_\zeta(x)$ is the PDF of PU received signal strength (RSS) ζ (e.g. TV signal). The outage rate of PU should be acceptable:

$$Pr\left(\gamma \leq \gamma_{min}\right) = O_{max} \ , \tag{10}$$

where γ_{min} and O_{max} are the allowed minimum SIR and maximum outage probability for PU, respectively. From (9) and (10), the SU transmit power p' can be found as:

$$p' = \min\left\{\gamma_{min}\zeta F_\gamma^{-1}(O_{max}), p'_{max}\right\} \ , \tag{11}$$

where p'_{max} is the maximum allowable transmit power, and $F_\gamma(x)$ is the CDF of SIR at an arbitrary PU receiver.

D. Efficient Computation Approach

Based on the logarithmic random interference Y in (2), where $L(d)$, P and H are independent r.v.s, the PDF of Y can be found by chained convolutions [21]:

$$f_Y(Y) = \left[(f_L * f_H) * f_P\right](Y) \ , \tag{12}$$

where f_L, f_P, and f_H, are the PDFs of logarithmic path gain, emission power, and the underlying normal distribution of log-normal fading, respectively. Similarly, the PDF of logarithmic SIR, Γ, can be found by:

$$f_\Gamma(\Gamma) = (f_Z * f_{-U})(\Gamma) \ , \text{where } f_{-U}(x) = f_U(-x) \ , \tag{13}$$

and f_Z and f_U are the PDFs of logarithmic TV signal RSS and aggregated Interference, respectively.

The PDF of linear domain random interference $f_y(x)$ is obtained from (12) with a down-sampled interpolation, e.g. a down-sample rate of 10^5 is used for the interested upper $70dB$ (for aggregate interference) out of the total dynamic range of 120dB. Required sample size in linear domain, n, is thus reduced from 10^{12} to 10^7. PDF of linear aggregate interference $f_u(x)$ is obtained by applying $\Phi_y(w) = \mathcal{F}\left\{f_y(x)\right\}(w)$, (4), and $f_u(x) = \mathcal{F}^{-1}\left\{\Phi_u(w)\right\}(x)$, which has a complexity of $\mathcal{O}(n\log(n))$. Reducing n from 10^{12} to 10^7 can reduce the computational complexity by 50,000 times. Logarithmic power control has a complexity of $\mathcal{O}(\ln(n))$ instead of $\mathcal{O}(n)$ for linear domain. In Section V, this approach is shown to preserve the precision of high quantiles of the estimated CDFs, which are vital to outage analysis and power control.

V. Simulation Results

The developed model (*Model*) is evaluated by simulation of a circular region with radius $R = 3,000m$. In the simulation, PUs and SUs are generated by homogeneous PPPs with specified densities. SU admission ratio is set to 100%. SUs in the guard zones of PUs are firstly removed, then a random contention keeps only one SU out of multiple SUs in a contention zone [11]. Radiuses of guard zone and contention zone are $100m$ and $20m$, respectively. The reference transmit power of SU is 16 dBm [1]. Propagation model of secondary signal is ITU-R P.1411 with a path loss exponent of 4, and logarithmic fading $\sim \mathcal{N}(0, (7.6dB)^2)$. Logarithmic RSS of TV signal in the region is assumed to follow a Normal distribution $\mathcal{N}(-56dBm, (4.7dB)^2)$. The center frequency is set to $623MHz$ (channel 39 in the U.S.). Allowable minimum SIR for TV receiver $\gamma_{min} = 23dB$, and maximum outage rates, $O_{max} \in \{0.1, 0.05, 0.01\}$, are used in power control. TV RSS, individual and aggregated interference at the origin point are collected. Each simulation contains 10,000 instances.

The model is benchmarked by 3 common lognormal approximations with low computational complexity:

1) *Analytical Approximation (Approx.)*: The first two moments are found via Compbell's Theorem [18], based on the PDF of random interference from (5), and thinned PPP in (7). The precision is impacted by the PPP approximation of PHP and computational dynamic range.
2) *Empirical Fitting (Fitting)*: The first two moments are from simulated empirical data. It can represent measurement-based estimation, and reflect how far the empirical interference is distorted from lognormal.
3) *Extreme Location Analysis (Extreme Loc.)*: Interference from a transmitter at a prescribed minimum distance, in this case, r_p. Attenuation includes fading and a fixed path loss. It is a well-accepted simplification [3], [4].

We compare the estimation accuracy, outage rate of PU, and SINR loss of SU in power control in the following.

A. Model Accuracy Under Network Dynamics

1) Homogeneous Secondary Users: Each SU is equipped with an omni-directional antenna of 0dBi gain, and transmit power of 16dBm. 24 network conditions from the combinations of PU densities $\{1, 10, 150\}/km^2$, and SU densities $\{40, 80, 120, 160, 200, 240, 280, 320\}/km^2$ are simulated. The dynamic range of aggregate interference in these configurations is -120 to -55dBm, and -180 to -80dBm for random individual interference. The CDFs of aggregate interference from simulation and estimations under 3 conditions, HPLS (High PU density, Low SU density), HPHS, and LPHS, are presented in Fig. 3(a). The median interferences of HPLS, HPHS, and LPHS, are 15 and 16dB apart, respectively, since PU reduces the spectrum opportunity of SUs. The Model is accurate in high quantiles (as shown in Fig. 3(c) and discussed later) while introducing a large error ($> 1dB$) in lower quantile ($F(x) \leq 0.6$ for HPLS, $F(x) \leq 0.3$ for HPHS) (circled in Fig. 3(a)) due to the approximation of PHP, and limits of computational dynamic range (-120 to -50dBm).

2) Heterogeneous Secondary Users: This setting contains 2 classes of SUs: Class 1 is configured the same as Section V-A1. Class 2 SU is equipped with a 4-antenna array. The densities of SU and PU are fixed to 200 and $20/km^2$, respectively. We evaluate 30 combinations from class 2 SU proportions $\{0, 0.25, 0.5, 0.75, 1\}$, transmit power $\{10, 16, 20\}\,dBm$, and stream numbers $\{1, 4\}$. Detailed CDFs of interference from

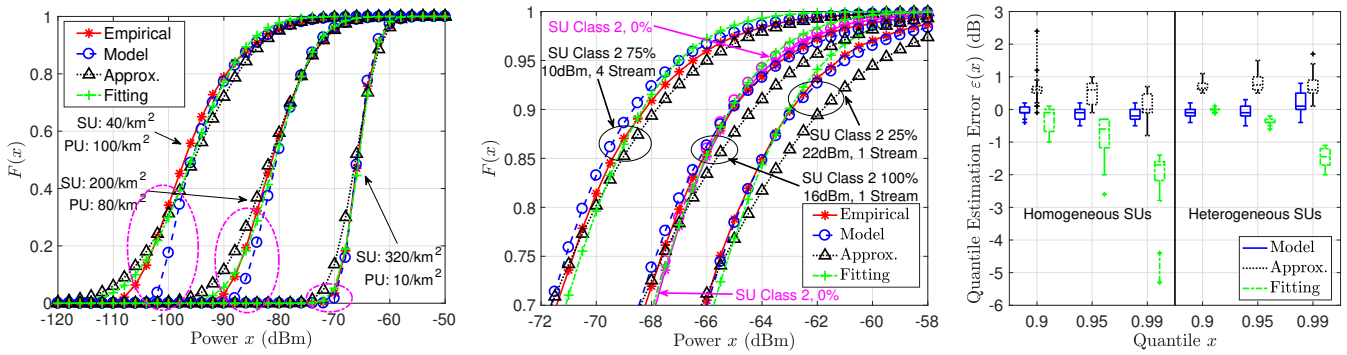

(a) (b) (c)

Fig. 3. Aggregate interference: (a) CDFs for homogeneous SUs, (b) zoomed-in CDFs for heterogeneous SUs, and (c) estimation errors at quantiles $\{0.9, 0.95, 0.99\}$.

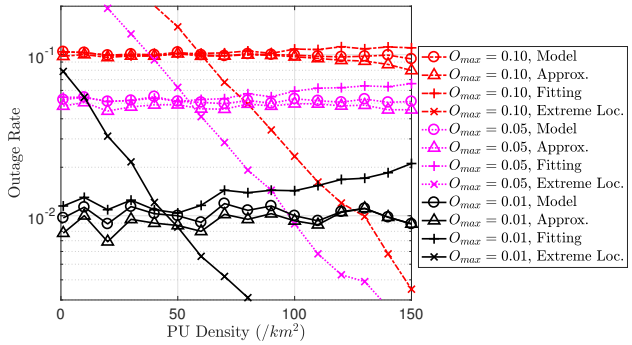

Fig. 4. PU outage rate by PU density under power control.

simulation and estimations for 4 SU composites is presented in Fig. 3(b). In the case of 75% SUs are in class 2, with 4 streams, and transmit power of 10 dBm, interference is reduced for about 3.7dB from the reference case (100% class 1 SU) which allows more SUs to be admitted. In the case of 25% SUs are in class 2, with 1 stream and transmit power of 22 dBm, interference increases by about 2dB from the reference case. When all SUs are class 2, with 1 stream and identical transmit power of reference case, the interference is very close to reference case. In Fig. 3(b), aggregate interference is shown to be dominated by transmit power, however, antenna array causes stronger spurious interference in high quantile ($F(x) > 0.95$) despite it lowers the median interference. Moreover, in the case of 25% SU class 2 in Fig. 3(b), with interference power of -60dBm, the outage rates from simulation, Model, Approx., and Fitting are 3%, 3.5%, 10.4%, and 1.5%, respectively. Outage rates predicted by lognormal approaches are 346% and 50% of the simulation.

The precisions of model and benchmarks over large dynamics of densities of PU and SU (homogeneous SUs) and SU composites (heterogeneous SUs) are evaluated via quantile estimation error, $\varepsilon(x) = F_{est}^{-1}(x) - F_{sim}^{-1}(x)$, where $x \in \{0.9, 0.95, 0.99\}$, and F_{est} and F_{sim} are CDFs from estimation and simulation, respectively. The results are presented in Fig. 3(c), with Root Mean Squares (RMS) in Table I. Analytical approximation over-estimates the interference for 0.7 dB on average with the worst error $\varepsilon(0.9) = 2.4dB$ for homogeneous SUs. Empirical fitting generally underestimates the interference, with significant high quantile errors (Worst: $\varepsilon(0.95) = -2.6dB$, $\varepsilon(0.99) = -5.3dB$). The Model consistently keeps RMS $< 0.28dB$ for all 3 quantiles except a slight increase to $0.38dB$ at quantile 0.99 in heterogeneous SUs.

Table I. Root Mean Square Estimation Errors at High Quantiles (Unit: dB)

Setting	Homogeneous SUs			Heterogeneous SUs		
Quantile	0.9	0.95	0.99	0.9	0.95	0.99
Model	**0.22**	**0.28**	**0.27**	0.17	**0.20**	**0.38**
Approx.	0.77	0.63	0.39	0.72	0.86	0.77
Fitting	0.46	1.04	2.30	**0.05**	0.39	1.49

In MATLAB, finding CDFs via (4) (shared by [10]–[17]) is intractable for dynamic range $\geq 90dB$. However, by tracking the upper 70 (80) dB out of 120dB range, our approach takes 0.78 (20) sec for a single SU class, and 1.57 (41) sec for 2 SU classes. *Approx.* (*Fitting*) only takes 0.21 (<0.001) sec.

B. Power Control Performance

Power control in (11) is evaluated under PU densities 1–150$/km^2$ (e.g. varying hourly TV usage) and SU density of 200$/km^2$. p'_{max} is not applied for comparison purpose. The model keeps PU outage rate (Fig. 4) in $\pm 5\%, 10\%, 19\%$ of required rates of 0.1, 0.05, 0.01, respectively. Compared to simulation-based ideal power control, the model only loses SU SINR for $\pm 0.3dB$. *Fitting* generally under-protects PU, with the worst outage rate twice of required (0.01). *Approx.* generally over-protects PU by sacrificing SU SINR (up to 2.3 dB). Performance loss due to lognormal approaches is significant. Constant power (Extreme Loc.) either under-protects (low PU density) or overprotects (high PU density) PU by sacrificing SU SINR (up to 15dB for the highest PU density).

VI. Experimental Evaluation

The core modeling component in (4) is validated by an experiment of aggregating WiFi beacons in a residential area. We choose this experiment because WiFi access points (APs) in a residential area are unplanned and accessible. Each AP broadcasts beacon frame every 100ms under CSMA/CA mechanism. Each received beacon can be viewed as an independent collision-free transmission. Moreover, received beacon carries the identity (SSID), number of streams (for MIMO AP), and working band of its transmitter. The RSS and SNR of the received beacons are measured by the receiver.

We collect beacons of nearby WiFi APs at 50 locations in a residential area in the U.S. (Fig. 5(a)), where buildings are mostly of 2–4 floors with wooden and brick structures.

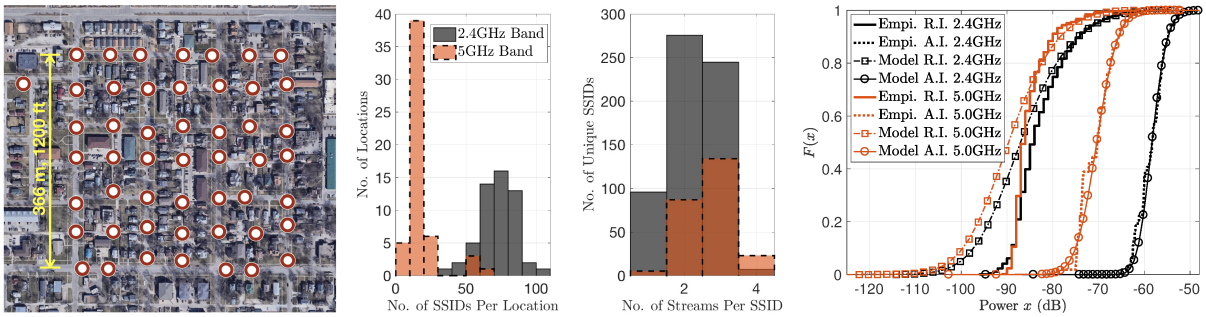

(a) (b) (c) (d)

Fig. 5. Experiments: (a) Locations, histograms of (b) SSIDs per location, (c) streams per unique SSID, (d) CDFs of random interference (R.I.) and aggregate interference (A.I.). from empirical data (Empi.) and models.

At each location, a laptop with *WiFi Scanner* [22] updates received beacons every 5 seconds, and lasts for a minute so that no AP is missed. The histograms of the number of SSIDs per location, and the number of streams per unique SSID, are shown in Figs. 5(b) and 5(c), respectively. On average, an SSID in the 2.4GHz (5GHz) band has 2.26 (2.70) streams.

An individual beacon is treated as a random interference (R.I.), and the empirical aggregate interference (A.I.) at each location is the sum of all R.I.s in each band. Next, R.I. and A.I. are estimated via (5) and (4), respectively. For the parameters, r_p is set to $18m$ (half of the average width of streets), without other PU. R is selected as $90m$ for 2.4GHz band, and $64m$ for 5GHz. AP transmit power is assumed to 36dBm. Modified ITU-R. P1411, with a 40dB gain bias, and logarithmic fading $\sim \mathcal{N}(0, (4.6dB)^2)$, is used as the propagation model. $\lambda_t c$ in (4) is set as the average number of SSIDs per location, 72.2 (17.2) in the 2.4GHz (5GHz) band. The distributions of R.I. and A.I. of all locations in 2.4GHz and 5GHz bands are shown in Fig. 5(d). Limited by receiver sensitivity, empirical R.I. at lower quantiles is significantly less than the model. However, the empirical A.I. and model in both 2.4 and 5GHz bands are well matched (RMS horizontal gaps of 0.17dB (2.4GHz) and 0.19dB (5GHz) in upper quantiles $F(x) \geq 0.5$). The results show that with correct average number of SU transmitters, the underlying model in (4), which is also shared by [10]–[17], can predict interference with high accuracy in upper quantiles.

VII. Conclusion

In this paper, we modeled the aggregate interference in cognitive radio networks with unplanned primary users and co-located secondary users with heterogeneous power and MIMO profiles, and provided an efficient computation approach. Simulation shows the model has limited high-quantile error (-0.5–0.8dB) over large network dynamics. Moreover, the core stochastic geometry modeling component is validated experimentally. With the model, interference to PU can be managed by adaptively limiting SU density and transmit power, which can potentially enhance future TV spectrum access.

Acknowledgment

This work is supported by US National Science Foundation grant NSF CNS 1731833.

References

[1] "Third memorandum opinion and order," FCC., Sep 2012.

[2] S. Bhattarai, J. M. J. Park, B. Gao, K. Bian, and W. Lehr, "An overview of dynamic spectrum sharing: Ongoing initiatives, challenges, and a roadmap for future research," *IEEE Trans. on Cognitive Commun. and Netw.*, vol. 2, no. 2, pp. 110–128, June 2016.

[3] K. Harrison, S. Mishra, and A. Sahai, "How much white-space capacity is there?" in *IEEE DySPAN*, Apr. 2010, pp. 1–10.

[4] Z. Zhao, M. C. Vuran, D. Batur, and E. Ekici, "Ratings for spectrum: Impacts of TV viewership on TV whitespace," in *IEEE GLOBECOM 2014*, Dec 2014, pp. 941–947.

[5] I. F. Akyildiz, W.-Y. Lee, M. C. Vuran, and S. Mohanty, "NeXt generation/dynamic spectrum access/cognitive radio wireless networks: A survey," *Comput. Netw.*, vol. 50, no. 13, pp. 2127–2159, Sep 2006.

[6] B. Gao and et al, "Incentivizing spectrum sensing in database-driven dynamic spectrum sharing," in *IEEE INFOCOM*, April 2016, pp. 1–9.

[7] X. Zhang and E. W. Knightly, "Watch: Wifi in active tv channels," in *ACM MobiHoc '15*. New York, NY, USA: ACM, 2015, pp. 7–16.

[8] R. Chernock and J. C. Whittaker, "Next-generation broadcast television: Atsc 3.0 [standards in a nutshell]," *IEEE Signal Processing Magazine*, vol. 33, no. 1, pp. 158–162, Jan 2016.

[9] D. Xue, E. Ekici, and M. C. Vuran, "Cooperative spectrum sensing in cognitive radio networks using multidimensional correlations," *IEEE Trans. on Wireless Commun.*, vol. 13, no. 4, pp. 1832–1843, April 2014.

[10] M. Win, P. Pinto, and L. Shepp, "A mathematical theory of network interference and its applications," *Proc. of the IEEE*, vol. 97, no. 2, pp. 205–230, Feb 2009.

[11] Z. Chen and et.al., "Aggregate interference modeling in cognitive radio networks with power and contention control," *IEEE Trans. on Commun.*, vol. 60, no. 2, pp. 456–468, February 2012.

[12] C. han Lee and M. Haenggi, "Interference and outage in poisson cognitive networks," *IEEE Trans. on Wireless Commun.*, vol. 11, no. 4, pp. 1392–1401, April 2012.

[13] Z. Yazdanshenasan and et al, "Poisson hole process: Theory and applications to wireless networks," *IEEE Trans. on Wireless Commun.*, vol. 15, no. 11, pp. 7531–7546, Nov 2016.

[14] I. Flint, H. B. Kong, N. Privault, P. Wang, and D. Niyato, "Analysis of heterogeneous wireless networks using poisson hard-core hole process," *IEEE Trans. on Wireless Commun.*, vol. PP, no. 99, pp. 1–1, 2017.

[15] H. Elkotby and M. Vu, "Interference modeling for cellular networks under beamforming transmission," *IEEE Trans. on Wireless Commun.*, vol. 16, no. 8, pp. 5201–5217, Aug 2017.

[16] M. G. Khoshkholgh and V. C. M. Leung, "On the performance of mimo-svd multiplexing systems in hetnets: A stochastic geometry perspective," *IEEE Trans. on Veh. Tech.*, vol. 66, no. 9, pp. 8163–8178, Sept 2017.

[17] S. Kusaladharma and C. Tellambura, "Secondary user interference characterization for spatially random underlay networks with massive mimo and power control," *IEEE Trans. on Veh. Tech.*, vol. 66, no. 9, pp. 7897–7912, Sept 2017.

[18] J. Kingman, *Poisson Processes*. Encyclopedia of Biostatistics. 6., 2005.

[19] D. A. Basnayaka and H. Haas, "Mimo interference channel between spatial multiplexing and spatial modulation," *IEEE Trans. on Commun.*, vol. 64, no. 8, pp. 3369–3381, Aug 2016.

[20] M. J. Rahman and X. Wang, "Probabilistic analysis of mutual interference in cognitive radio communications," in *IEEE GLOBECOM*, Dec 2011, pp. 1–5.

[21] M. D. Springer, *The Algebra of Random Variables*. Wiley, 1979.

[22] "WiFi Scanner," 2017. https://www.accessagility.com/wifi-scanner